Production of light nuclei in Au+Au collisions from STAR BES-II

Sibaram Behera (for the STAR Collaboration)

Indian Institute of Science Education and Research (IISER) Tirupati, Tirupati–517619, India

Abstract

Two different models - the thermal model and coalescence model, which are based on distinct mechanisms - can be used to describe the production of light (anti-)nuclei in heavy-ion collisions. By analyzing the yields and ratios of the light (anti-)nuclei, we can gain valuable insights into their formation processes and the properties of the system at freeze-out. The enhancement in the compound ratios of light nuclei, such as $N_t N_p/N_d^2$ from the expected coalescence baseline, has been proposed as a tool to probe critical phenomena in the Quantum Chromodynamics phase diagram. The larger datasets collected by STAR during the second phase of the Beam Energy Scan program (BES-II) compared to BES-I ($\sim$ 10 times larger) and improved detector capabilities are expected to provide more precise measurements in extended kinematic coverage. In these proceedings, we will explore the centrality and energy dependence of the transverse momentum (p_T) spectra of d, and ^3He in Au+Au collisions across BES-II energies $\sqrt{s_{NN}}$ = 7.7 – 27 GeV. Additionally, we will report the centrality and energy dependence of the p_T integrated yields (dN/dy) and the mean p_T ($\langle p_T \rangle$) of light nuclei. Furthermore, we will discuss the centrality and p_T dependence of the coalescence parameters, B_A, with their broader physics implications.

Keywords: Heavy-ion collisions, particle yield, light nuclei, coalescence parameters

1. Introduction

Understanding the Quantum Chromodynamics (QCD) phase diagram of the strongly interacting matter is one of the main aspects of the heavy-ion collision experiments at the Relativistic Heavy Ion Collider (RHIC). Lattice quantum chromodynamics (LQCD) calculations and various QCD-based models have suggested that the transition between the quark-gluon plasma (QGP) and the hadronic matter is a smooth crossover at vanishing baryon chemical potential (μ_B), but likely changes to a first-order phase transition at large μ_B [1, 2]. The point at which the first-order transition ends in the temperature versus baryon chemical potential (T, μ_B) plane of the QCD phase diagram is called the critical end-point (CEP). Experimentally, the phase diagram can be explored by tuning the beam energy since the μ_B varies with the center-of-mass collision energy [3].

Exploring the QGP signatures, understanding the nature of phase transition, and identifying the conjectured CEP are the main aims of the Beam Energy Scan (BES) program at RHIC. Recently, it has been proposed that, based on the coalescence model, the light nuclei compound ratios, e.g. $N_t N_p/N_d^2$ and $N_{^4He} N_p/(N_{^3He} N_d)$ are sensitive to the neutron density fluctuations, and hence could serve as a potential probe of the critical phenomena in the QCD phase diagram [4]. Additionally, by studying the yields and yield ratios of the light (anti-)nuclei, we can gain a better understanding of their production mechanisms and the properties of the expanding system during freeze-out [5, 6].

In the first phase of the Beam Energy Scan (BES-I) program at RHIC, an enhancement relative to the coalescence baseline of the light nuclei yield ratio $N_t N_p/N_d^2$ was observed in the most central Au+Au collisions at $\sqrt{s_{NN}}$ = 19.6 and 27 GeV, with a combined significance of 4.1σ [7]. The precision of the new measurements will be significantly improved by the large data sets ($\sim$ 10$\times$ BES-I) obtained by the STAR BES-II with upgraded detector capabilities.

In these proceedings, the transverse momentum (p_T) spectra of d and ^3He in Au+Au collisions across BES-II energies $\sqrt{s_{NN}}$ = 7.7 – 27 GeV will be examined for various centrality and energy dependency. We will also present the mean p_T ($\langle p_T \rangle$) of light nuclei and the centrality and energy dependence of the p_T integrated yields (dN/dy). The centrality and p_T dependency of the coalescence parameters, B_A, along with their wider physics implications, will also be covered.

2. Analysis details

In this analysis, we use the Time Projection Chamber (TPC), which provides the average ionization energy loss per unit length ($\langle dE/dx \rangle$) and also provides tracking information and the Time of Flight (TOF) detectors give the particle's velocity (β) in STAR. Deuteron is identified using TPC information only up to p_T = 1.0 GeV/c, and above p_T = 1.0 GeV/c, d signal extraction is done by TPC+TOF. ^3He is identified by TPC only. The corrected light nuclei spectra can be obtained by implementing energy loss, TPC tracking efficiency, TOF matching efficiency, and knockout corrections. The systematic uncertainties on each p_T bin in the spectra can be estimated by varying the analysis cuts. The systematic uncertainties of dN/dy and $\langle p_T \rangle$ are estimated by considering the uncertainties in each p_T bin in the spectra and the deviation between the extrapolated range of the Blast-Wave model and double p_T function fits to the p_T spectra.

3. Results

3.1. Corrected p_T spectra

The p_T spectra of deuterons and ^3He in Au+Au collisions from the STAR BES-II program are shown in Fig. 1 and Fig. 2, respectively. We have measured p_T spectra in finer centrality and finer p_T bins due to the availability of high statistics BES-II data sets. Additionally, due to STAR detector's upgrades, we have inner TPC (iTPC), which provides better p_T acceptance and extended p_T ranges. As a result, there is a reduction in the systematic uncertainties of the particle yields in BES-II energies.

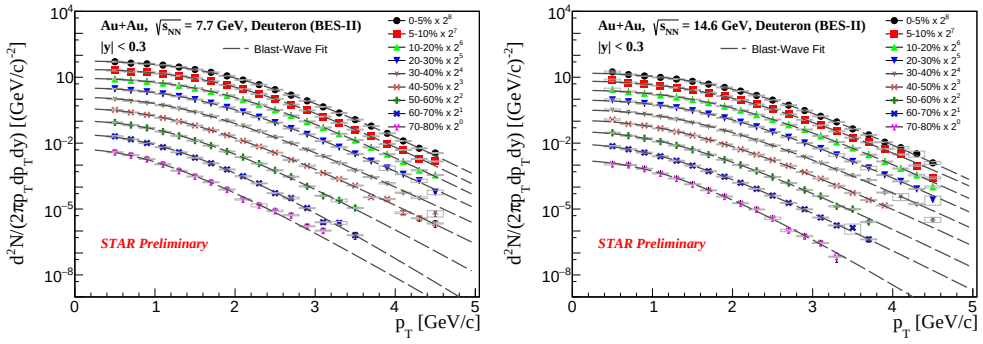

(a) (b)

Figure 1: The p_T spectra of the d at mid-rapidity ($(|y| \leq 0.3)$) in various centralities in Au+Au collisions at $\sqrt{s_{NN}}$ = 7.7 and 14.6 GeV is shown. The dashed lines represent the Blast-Wave fits. Statistical and systematic uncertainties are shown as vertical bars and boxes, respectively.

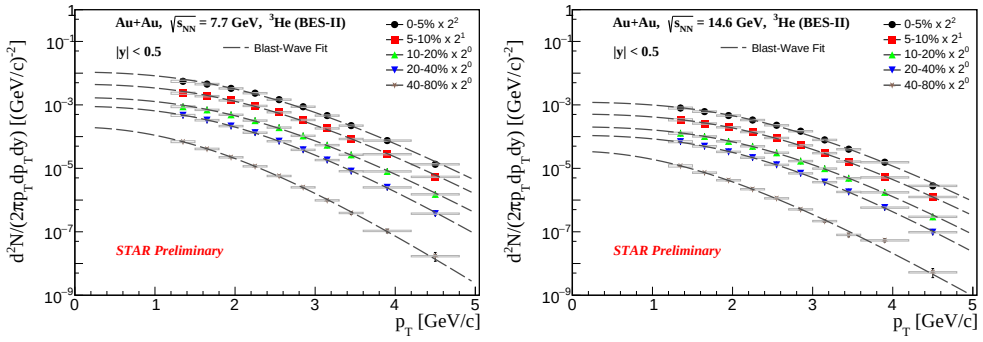

(a) (b)

Figure 2: The p_T spectra of the ^3He at mid-rapidity ($|y| \leq 0.5$) in various centralities in Au+Au collisions at $\sqrt{s_{NN}}$ = 7.7 and 14.6 GeV is shown. The dashed lines represent the Blast-Wave fits. Statistical and systematic uncertainties are shown as vertical bars and boxes, respectively.

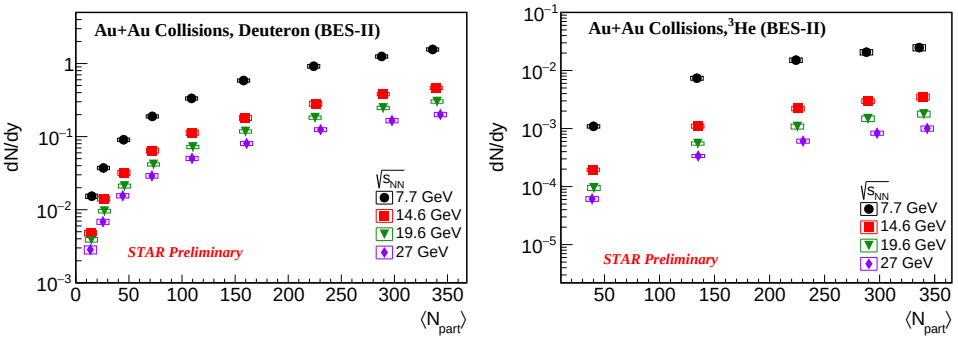

(a) (b)

Figure 3: The dN/dy of d (left) and ^3He (right) in Au+Au collisions at $\sqrt{s_{NN}}$ = 7.7 – 27 GeV are shown. Statistical and systematic uncertainties are shown as vertical bars and boxes, respectively.

3.2. Light nuclei yield (dN/dy)

The dN/dy of the light nuclei are calculated from the measured p_T spectra by integrating over p_T, and the extrapolation is done by Blast-Wave model fits. The dN/dy of d and ^3He at BES-II energies as a function of $\langle N_{part}\rangle$ are shown in Fig. 3. Here, $\langle N_{part}\rangle$ serves as a proxy of collision centrality. We have observed that the decrease in dN/dy from central to peripheral collisions suggests that the energy density is higher in central collisions. The yield decreases with increasing collision energies due to the stronger baryon stopping effect at lower collision energies as compared to higher collision energies.

3.3. Light nuclei mean transverse momentum ($\langle p_T\rangle$)

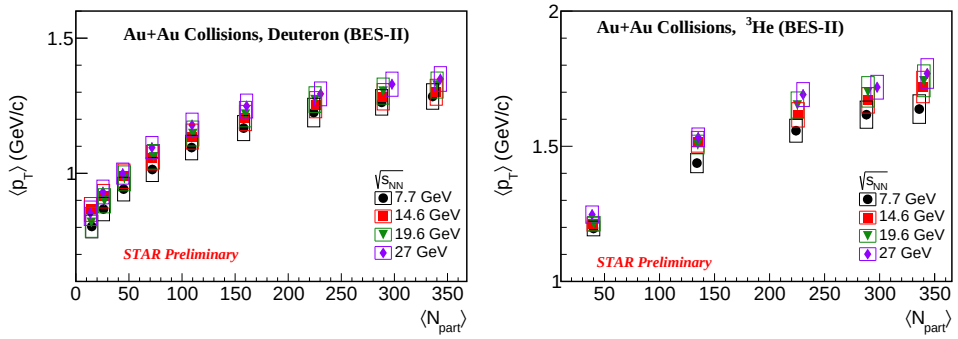

(a) (b)

Figure 4: The $\langle p_T\rangle$ of d (left) and ^3He (right) in Au+Au collisions at $\sqrt{s_{NN}}$ = 7.7 – 27 GeV are shown. Statistical and systematic uncertainties are shown as vertical bars and boxes, respectively.

The $\langle p_T\rangle$ of light nuclei are also extracted from the measured p_T range, and extrapolations of the Blast-Wave model fit to the p_T spectra. The $\langle p_T\rangle$ of d and ^3He at BES-II energies as a function of $\langle N_{part}\rangle$ are shown in Fig. 4. We observe that it increases with increasing centrality due to larger radial flow in central collisions. Furthermore, at a given collision centrality, the $\langle p_T\rangle$ of light nuclei is comparable at various collision energies.

3.4. Coalescence parameters (B_A)

$$E_A\frac{d^3N_A}{dp_A^3} = B_A(E_p\frac{d^3N_p}{dp_p^3})^Z(E_n\frac{d^3N_n}{dp_n^3})^{A-Z} \approx B_A(E_p\frac{d^3N_p}{dp_p^3})^A \quad (1)$$

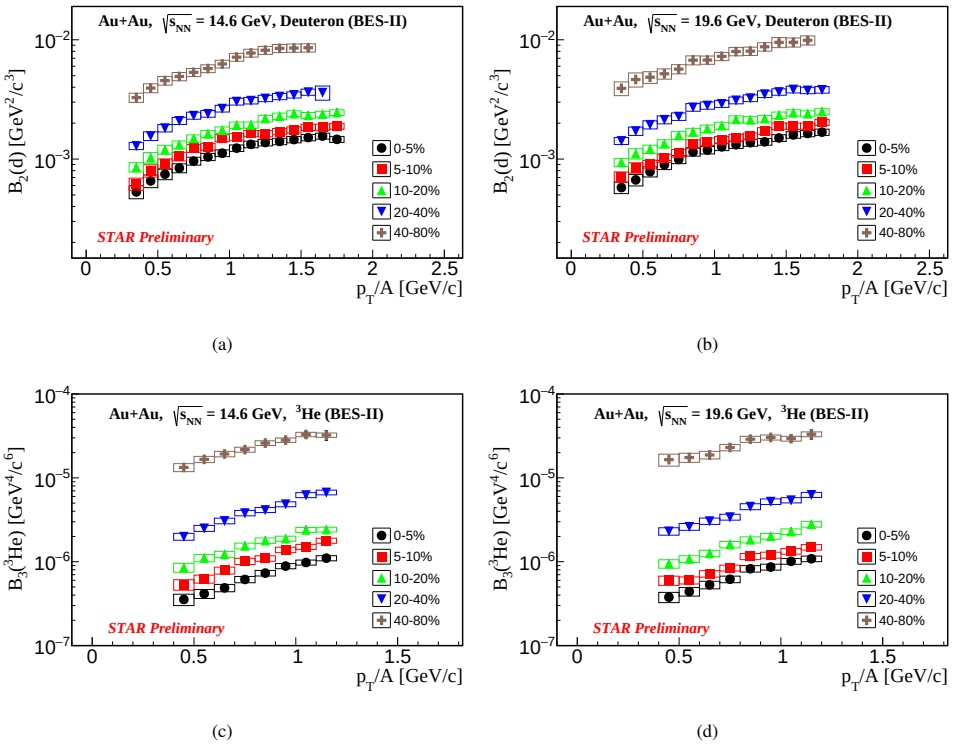

Figure 5: The p_T dependence of B_2 (upper panel) and B_3 (lower panel) with number of constituent nucleons scaling for deuteron and ^3He at various centralities in Au+Au collisions at $\sqrt{s_{NN}}$ = 14.6 GeV (left) and 19.6 GeV (right) are shown. Statistical and systematic uncertainties are shown as vertical bars and boxes, respectively.

The invariant yield of light nuclei in the coalescence picture is proportional to the invariant yield of nucleons, as given by Eq. 1. Here, $p_A = Ap_p$ and A, Z are the mass number and charge number of the light nuclei. p_A, p_p, and p_n are the momenta of the nucleus, proton, and nucleon, respectively. In this case, neutron-to-proton ratio is assumed to be unity. The likelihood of nucleon coalescence is reflected in the coalescence parameters B_A and is correlated with the local nucleon density. Figure 5 shows B_A as a function of p_T/A across various centralities at $\sqrt{s_{NN}}$ = 14.6 and 19.6 GeV. B_A is seen to rise with p_T/A, which may indicate an expanding collision system. B_A is larger in peripheral than in central collisions, which is explained by a decreasing source volume.

4. Summary

The p_T spectra of light nuclei are measured in Au+Au collisions at BES-II energies of $\sqrt{s_{NN}}$ = 7.7 – 27 GeV. The dN/dy of deuterons and ^3He are observed to decrease from central to peripheral collisions and decrease with increasing collision energy. The $\langle p_T \rangle$ of light nuclei increases with increasing collision centrality and is comparable at a given $\langle N_{part} \rangle$ across different energies. The B_A increases with increasing p_T/A and is larger in peripheral collisions.

References

[1] Z. Fodor, S.D. Katz, J. High Energy Phys. **0404**, 050 (2004).
[2] M. Asakawa, K. Yazaki, Nucl. Phys. A **504**, 668 (1989).
[3] J. Cleymans, H. Oeschler, K. Redlich, and S. Wheaton, Phys. Rev. C **73**, 034905 (2006).
[4] K.J. Sun, L.W. Chen, C.M. Ko, Z. Xu, Phys. Lett. B **774**, 103 (2017).
[5] J. Adam *et al*. [STAR Collaboration]. Phys. Rev. C. **99**, 064905 (2019).
[6] W. Zhao, C. Shen, C. M. Ko, Q. Liu, and H. Song, Phys. Rev. C **102**, 044912 (2020).
[7] M. I. Abdulhamid *et al*. [STAR Collaboration]. Phys. Rev. Lett. **130**, 9 (2023).